NJC

Accepted Manuscript

This is an *Accepted Manuscript*, which has been through the Royal Society of Chemistry peer review process and has been accepted for publication.

Accepted Manuscripts are published online shortly after acceptance, before technical editing, formatting and proof reading. Using this free service, authors can make their results available to the community, in citable form, before we publish the edited article. We will replace this *Accepted Manuscript* with the edited and formatted *Advance Article* as soon as it is available.

You can find more information about *Accepted Manuscripts* in the Information for Authors.

Please note that technical editing may introduce minor changes to the text and/or graphics, which may alter content. The journal's standard Terms & Conditions and the Ethical guidelines still apply. In no event shall the Royal Society of Chemistry be held responsible for any errors or omissions in this *Accepted Manuscript* or any consequences arising from the use of any information it contains.

ROYAL SOCIETY OF CHEMISTRY

www.rsc.org/njc

Enzyme immobilization and molecular modeling studies on organic-inorganic polypyrrole-titanium(IV)phosphate nanocomposite

Umair Baig[a,b]*, Mohammed Ashraf Gondal[a,b]*, Md Fazle Alam[c], Amaj Ahmed Laskar[c] Mahboob Alam[d], Hina Younus[c],

[a]*Center of Excellence for Scientific Research Collaboration with MIT, King Fahd University of Petroleum and Minerals, Dhahran 31261, Saudi Arabia*

[b]*Laser Research Group, Physics Department & Center of Excellence in Nanotechnology King Fahd University of Petroleum and Minerals, Dhahran 31261, Saudi Arabia*

[c]*Interdisciplinary Biotechnology Unit, Aligarh Muslim University, Aligarh-202002 (UP) India*

[d]*Division of Bioscience, Dongguk University, Gyeongju 780-714, Republic of Korea*

*Corresponding authors' email: **umairbaig@kfupm.edu.sa** **(U. Baig)**

magondal@kfupm.edu.sa **(M.A.Gondal)**

Telephone: +9663-8602351/8603274; *Fax:* +9663-8604281

Abstract: In this work we report the synthesis of electrically conductive polypyrrole-titanium(IV)phosphate (PPy-TiP) nanocomposite using simple, facile *in-situ* chemical oxidative polymerization of polypyrrole (PPy) in the presence of titanium(IV)phosphate (TiP) for immobilization of yeast alcohol dehydrogenase enzyme. FTIR, FE-SEM and TGA were employed in the characterization of PPy, TiP and PPy-TiP nanocomposite. YADH was successfully immobilized on PPy-TiP nanocomposite with loading efficiency of 69%. The immobilized YADH has shown no change in the pH optima (pH-8.0) and there was a broadening of the peak both in acidic as well as in alkaline pH. The optimum temperature of immobilized YADH was increased by 5 ^{o}C with almost the same residual activity. Immobilized YADH has shown improved thermal stability at 60 ^{o}C and retained about 71% activity after 5 h of incubation. Also, the immobilized YADH has shown greater reusability and retained 75% activity after 10th successive use. All the results were compared to that of free YADH, immobilized YADH on PPy and immobilized YADH on TiP. The affinity of immobilized YADH for ethanol was decreased as evident from the Km value (223.71 mM) and also there was a decrease in the maximum velocity (201.53 μM/min) as compared to soluble YADH. The improved residual activity, stability and reusability of YADH immobilized on PPy-TiP nanocomposite makes the enzyme more suitable for industry-based applications. Molecular docking was used to query the protein– the newly synthesized chemical entities interactions that help in understanding the affinity in enzyme activity.

Keywords: Nanocomposite; Immobilization; Yeast Alcohol dehydrogenase.

1. Introduction

Electrically conductive polymers such as polyacetylene, polyaniline, polypyrrole, polythiophene, polycarbazole etc. have been extensively studied due to their excellent properties and a lot of applications in different areas.[1-9] Amongst these polymers, polypyrrole (PPy) has been widely utilized for enzyme immobilization due to high electrical conductivity, biocompatibility and facile synthesis at low cost in comparison to other polymers.[10-11] Poor mechanical and thermal stabilities are the major negative aspects which restrict their use in biotechnology and biomedical applications. To solve these problems, the nanocomposite of PPy with stable nanoparticles are expected to show higher thermal and mechanical stability due to synergism between the constituents.[12] Recently, the utilization of titanium based nanoparticles has risen as a versatile tool for creating fantastic supports for enzyme stabilization because of their small size and extensive surface area. Titanium based nanoparticles unequivocally impact the mechanical and thermal properties of the material like firmness and flexibility and give a bio-compitable environment for enzyme immobilization. The literature survey reveals that the titanium phosphates are highly porous and amphoteric material.[13] Owing to the beneficial properties of both PPy and TiP, the composite of PPy with TiP is expected to prove as an effective material for the enzyme immobilization.

Alcohol dehydrogenases (ADH) catalyze the NAD(P)-dependent oxidation of alcohols to their corresponding aldehydes or ketones and vice versa. They are found in plants, animals, yeast and microbes and are important enzyme for alcohol metabolism, generation of NAD(H).[14-15] YADH has been used widely in industries for the production of stereospecific organic compounds, pharmaceuticals, fine chemicals, industrially useful starting materials, fermentation products

etc.[16-18] As biosensor, Yeast alcohol dehydrogenase (YADH) entrapped within polymer has been used for the detection of ethanol.[19] Such potential applications of this enzyme are limited by its low stability, limited reusability and difficulty in recovery.[20-21] Many strategies were made previously to increase the stability of industrial enzymes which includes covalent modification, use of stabilizers, entrapment into polymers and immobilization.[22-23] In many instances, immobilized enzymes have shown improved stability, recovery and reusability.[24] YADH has been previously immobilized on nanomaterials such as silver nanoparticles, magnetic nanoparticles, alginate-chitosan beads etc.[21, 25] and have shown significant increase in stability, recovery and reusability. In this study, we have immobilized YADH on PPy-TiP nanocomposite using CNBr and compared its stability, recovery and reusability with that of free enzyme as well as that immobilized on PPy and TiP separately. Finally, interactions between ADH and the newly synthesized chemical entities were studied using in-silico structure based molecular docking methods. It involves evaluating quick calculation of the most favorable interaction between different entities and hence coherent designing of nanocomposite for desired properties.

2. Experimental

2.1. Chemicals and reagents

The following reagents were used in this study. Pyrrole monomer (98%), anhydrous iron(III)-chloride ($FeCl_3$), methanol (HPLC grade) ortho-phosphoric acid (H_3PO_4), titanium dioxide (TiO_2), ammonium sulphate, acetonitrile and cyanogen bromide (CNBr) obtained from Sigma-Aldrich was used as received.

2.2. Synthesis

2.2.1. Titanium(IV)phosphate

TiP was prepared by simple precipitation technique from aqueous solutions of titanium(IV)sulfate and H_3PO_4. Titanium(IV)sulphate solution was prepared as has been described in our previous publications.[26-27] With vigorous stirring, aqueous solution of H_3PO_4 was added dropwise in titanium(IV)sulfate solution. The mixture was stirred for 24h at 25 ºC to form an absolute precipitate. After 24 h, resulting precipitate was filtered off, washed with demineralized water (DMW) and dried at 100 ^oC for 24h. Finally, the material was ground by pastel mortar to yield a fine TiP powder.

2.2.2. Polypyrrole-titanium(IV)phosphate nanocomposite

In-situ oxidative chemical polymerization[7-9] of pyrrole with $FeCl_3$ as the oxidizing agent, in the presence of TiP particles, was used in the preparation of the nanocomposite (PPy-TiP). A definite amount of TiP was dispersed in 100 mL of DMW under ultrasonic vibrations at 25 ^oC for 1 h. The dispersed TiP solution was then poured into a 500 mL round-bottom flask equipped with a magnetic stirrer and a definite amount of pyrrole (monomer) was added. For proper adsoption of pyrrole monomers on the TiP particles, vigorous stirring of the solutions for 4 hours was ensured. 2 g of $FeCl_3$ was dissolved in demineralized water (100 mL) and this $FeCl_3$ solution poured in the pyrrole adsorbed TiP dispersion. The reaction mixture was stirred for 24 h at 25 ºC. After 24 h, synthesized PPy-TiP nanocomposite was filtered and washed with DMW and methanol to remove unreacted oxidant. The obtained powders were dried completely at 70 ºC for further analysis. Pure PPy was synthesized by a similar method as the preparation of PPy-TiP nanocomposites without the TiP nanoparticles. A graphical demonstration of the development of PPy and PPy-TiP nanocomposite is indicated in **Fig. 1.**

2.3. Characterization

Perkin Elmer 1725 instrument was used in analyzing fourier transform infra-red spectroscopy (FTIR) spectra. Field emission scanning electron microscopy (FE-SEM) was carried out by LEO 435–VF to study the surface morphology. Thermal analyzer-V2.2A DuPont 9900 was used to investigate the thermal stability by analyzing the thermogravimetric analysis (TGA). Under nitrogen atmosphere at 200 mL/min flow rate, samples were heated (30-1000 ^{o}C) at the rate of 10 ^{o}C/min.

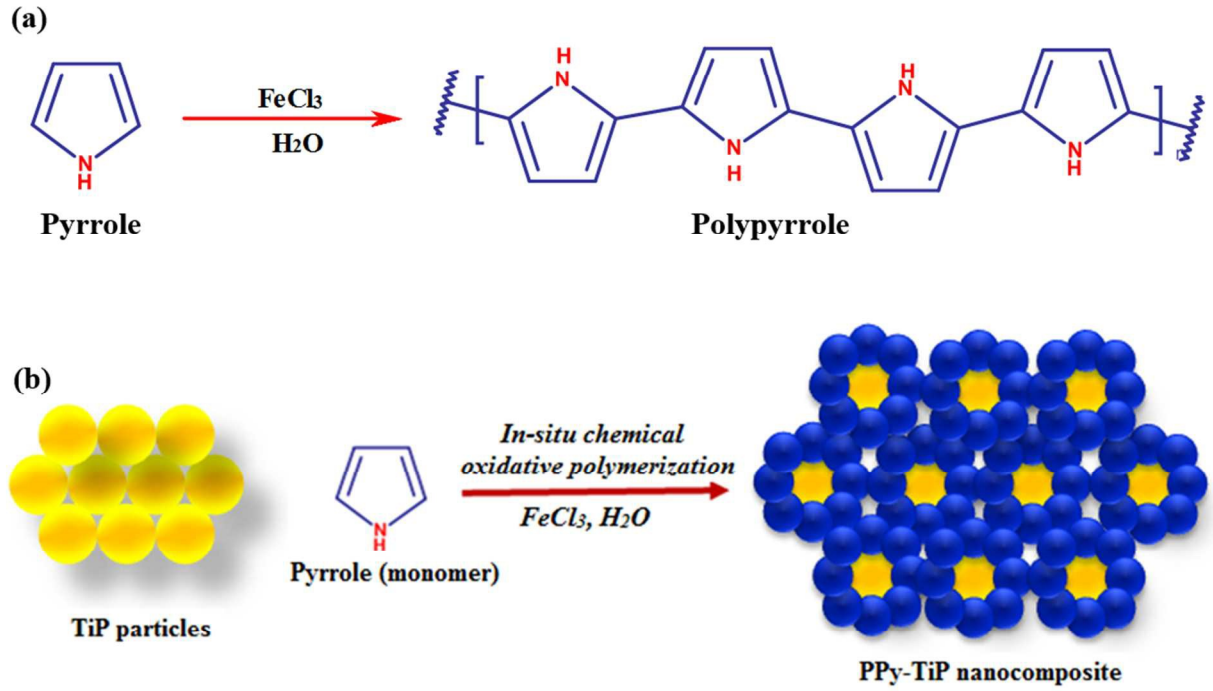

Fig. 1. Schematic diagram of the formation mechanism of (a) PPy and (b) PPy-TiP nanocomposite.

2.4. Enzyme immobilization studies

2.4.1. Activation of TiP and PPy-TiP nanocomposite with CNBr

Twenty milligrams each of PPy-TiP nanocomposite and TiP alone were taken separately and washed with distilled water in sintered funnel. 5 ml of distilled water, 5 ml of 2 M Na_2CO_3 and 1 gm of CNBr in 1 ml acetonitrile was added respectively to the PPy-TiP

nanocomposite and TiP. Both the solutions were kept stirring for 10 minutes at 4 **ºC**. The CNBr activated PPy-TiP nanocomposite and TiP were washed two times with 0.1 M bicarbonate buffer, pH-8.5 and with distilled water respectively in sintered funnel. The pellets obtained from both the preparations were then sucked dry and obtained nearly 18 mg of activated naocomposites and resuspended separately in 50 mM phosphate buffer of pH-7.4.

2.4.2. Immobilization of YADH to CNBr activated TiP and PPy-TiP nanocomposite

1 ml of 10 mg/ml solution of YADH was dissolved in 4 ml of 0.1M bicarbonate buffer, pH-8.5 and then the resulting solution (total 5 ml) was added each separately to 2 ml of 10 mg/mL CNBr activated PPy-TiP nanocomposite and TiP. The solutions were kept stirring at 4 **ºC** for 24 hours. Washing of the solutions was done repeatedly with 0.1 M Tris-HCl buffer, pH-8 by centrifugation at 2500 rpm for 5 minutes and resuspension of the pellets in Tris-HCl buffer. After washing five times, the absorbance at 280 nm of supernatant collected after each wash was measured in Shimazu UV1700 UV-VIS Spectrophotometer (Japan) and total amount of unbound YADH was estimated by using the formula A=E.c.l (Beer-Lambert Equation). Loading efficiency of YADH on nanocomposite was calculated as shown in supplementary file (See table S1). For PPy alone, the YADH was simply adsorbed on to the twenty milligrams of PPy in Tris-HCl buffer.

2.4.3. YADH activity assay

The activity assay of YADH was done using spectrophotometer for both soluble and immobilized enzyme with ethanol as substrate. Activity assay for soluble YADH was measured

using 100 µg of YADH in the presence of 0.1 M ethanol, 0.3 mM NAD^+ and 0.1 M Tris-HCl buffer, pH 8.0 in a total volume of 1 ml. After adding the substrate, the reaction mixture was incubated at 37 **ºC** and absorbance at 340 nm was taken after 3 min to measure the increase in NADH concentration. There were some modifications in case of immobilized YADH activity assay; in place of 1 mL of reaction mixture for soluble YADH, we used 3 mL of reaction mixture. From the loading efficiency and the effectiveness factor, we have calculated the amount of YADH immobilized per mg of nanocomposites and the active YADH in terms of enzyme unit. Appropriate amount of nanocomposite was then taken to get the desired amount of YADH in the reaction mixture. The standard reaction mixture of 3 mL contained desired amount of YADH immobilized nanocomposite (4.32 mg), 0.9 mM NAD^+ and 0.3 M of ethanol in 100 mM Tris-HCl buffer, pH 8.0. After incubating at 45 ^oC for 3 min, the reaction mixture was centrifuged and the supernatant was collected. The absorbance at 340 nm of the supernatant was measured as described above. A blank having all the above components, except the YADH was taken and was subtracted from the test.

2.4.4. Optimization of pH and temperature for immobilized YADH

Activity assay was done for soluble and immobilized YADH to optimize pH and temperature for the conversion of ethanol. pH optimization was done by measuring the activity of both enzyme preparations in different pH using 0.1 M buffers in the range of pH 3.0 to pH 12.0. The buffers used were glycine-HCl (pH 3.0), sodium acetate (pH 5.0), sodium phosphate (6.0, 7.0), Tris-HCl (pH 8.0, 9.0) and glycine-NaOH (pH 10.0, 12.0). The activity of YADH at pH 8.0 was considered as maximum (100%) to determine the percent activity at other pH.

Similarly, optimization of temperature was done by measuring the activity of soluble and immobilized YADH at different temperatures (25-70 **ºC**) in activity buffer of pH 8.0 (0.1 M

Tris-HCl) for 3.0 minutes. All the components used in this procedure are pre-heated at respective temperature for 15 min then used in the reaction mixture. The activity of YADH at 45 **ºC** was considered as maximum (100%) to determine the percent activity for both soluble and immobilized enzyme.

2.4.5. Thermal stability analysis

Analysis of thermal stability was done to determine the thermal stability of immobilized enzyme compared to free enzyme. For this, both free and immobilized enzyme preparations were incubated at 60 **ºC** for 5 hours. After every half an hour, starting from 0 hour, aliquots of the incubated enzyme were removed and chilled by placing in crushed ice for 5 minutes to bring down the temperature. The enzyme activity for each aliquot was then determined using the standard assay method as described above. The residual activity is expressed in relation to control which is the activity of the free enzyme without heating.

2.4.6. Analysis of reusability and recovery

The activity of immobilized YADH was measured after every use to determine its reusability and recovery. After each use, immobilized enzyme was recovered, washed and stored at 4 **ºC** and again used for 10 successive days. Washing was done in the activity assay buffer (0.1 M Tris-HCl buffer, pH 8.0) by centrifugation at 4000 rpm for 20 minutes and resuspending the pellet in the same assay buffer. The activity of immobilized YADH on the first day was taken as maximum (100 %) to calculate the remaining percent activity after each use.

2.5. In-silico studies

The retrieved protein associated with the yeast alcohol dehydrogenase (3BTO; pdb) was improved by the import and preparation option of the MVD software, and missing bond order, hybridization state, angle and flexibility to achieve reliable potential binding sites in the receptor.

The energy minimized PPy, activated TiP and activated PPy-TiP nanocomposite were drawn with ChemDraw Ultra (2D & 3D) and the prediction of their structural properties was conducted using the Discovery studio, MVD. For the purpose of molecular docking, tetramer of polymer is considered for the interaction between the protein and the compounds. These programs mentioned above were used to perform molecular docking and the energy profiles of ligand-receptor interactions were determined using the GEMDOCK program. The PARS, a web server, was used to predict the location of allosteric sites on enzyme structure for the successful docking at binding sites. These sites may cause a regulatory effect upon binding of the receptor when interacts with the guest.[28]

2.6. Field points studies

The structure of the PPy, activated TiP and activated PPy-TiP nanocomposite were drawn using Chem Draw Ultra 12.0 & Chem3D Pro 12.0 software and subsequently these structures were energetically minimized using MOPAC with MM2 and saved MDL molfile (*mol). Field points and geometrical descriptor were performed to identify the surface properties around the complexes using Torch Lite software of Cressetgroup (Cresset Biomolecular Discovery Ltd) and ChemAxon platforms.

3. Results and discussion

PPy-TiP nanocomposite was successfully prepared in a high yield of around 93.43%; by the polymerization of pyrrole *via* a facile *in-situ* chemical oxidative pathway in the presence of TiP. The nanocomposite showed efficient immobilization of YADH; an enzyme used in the synthesis of several industrially important aldehydes and alcohols. The immobilized YADH was bestowed with good thermal stability, and ability to work in harsh environmental (varied temperatures and pH) conditions.

3.1. FTIR spectroscopic studies

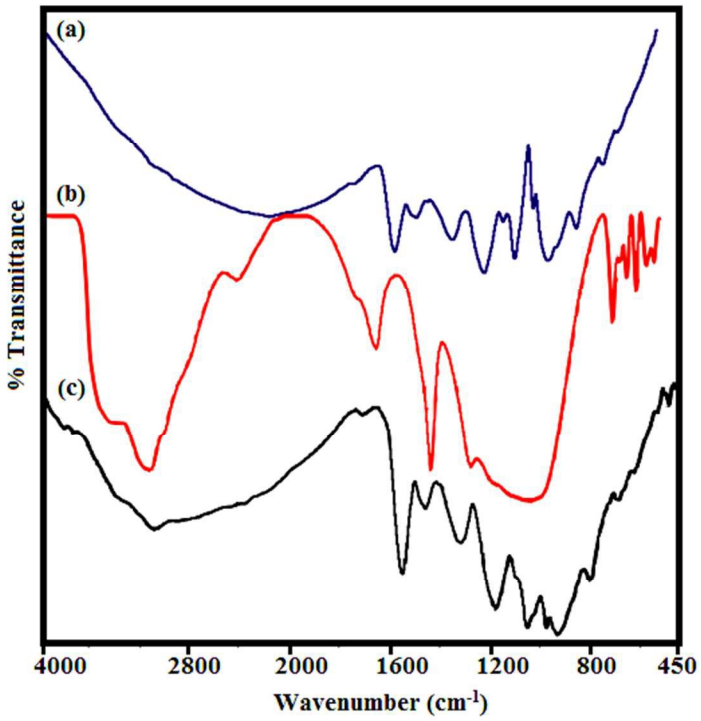

Fig. 2. FTIR spectra of (a) PPy (b) TiP and (c) PPy-TiP nanocomposite.

The FT-IR spectra of PPy, TiP and PPy-TiP nanocomposite are shown in **Fig. 2.** In the FT-IR spectrum of PPy, the characteristic absorption peak at 902 cm^{-1} corresponds to C–H out-of-plane deformation vibration; confirming the polymerization of pyrrole monomers into PPy polymer. The band at 1300 cm^{-1} is characteristic of C–N in-plane conformation. The bands at 1167 and 1041 cm^{-1} are attributed to the C–H bending modes while the strong absorption bands at 1539 and 1449 cm^{-1} corresponds to the C–C stretching vibration in the pyrrole ring. Additional peaks in the region of 600-1500 cm^{-1} are the characteristics of ring stretching and deformation of C–H in plane mode. The PPy-TiP nanocomposite exhibits positions of peaks similar to the main IR bands of PPy in the region of 450-4000 cm^{-1}. In comparison to the FTIR

spectra of PPy, the PPy-TiP displayed a strong band at 3089 cm^{-1} due –OH stretching frequency, and a broad band between 1250 and 900 cm^{-1} with a band intensity at 966 cm^{-1} due to the presence of ionic phosphate groups. Moreover, a peak at 790 cm^{-1} can be ascribed to M–O bonding. The peak at 1310 cm^{-1} in the FTIR spectrum of PPy-TiP shows the C–N stretching vibration thereby confirming the PPy polymerization on TiP particles.

3.2. Morphology of PPy, TiP and PPy-TiP nanocomposite

The FE-SEM images of PPy, TiP and PPy-TiP before and after immobilization of YADH are shown in **Fig. 3(a-c)** and **Fig. 3(a'-c')** respectively. **Fig. 3a** and **Fig. 3b** shows the morphology of PPy and TiP granules respectively. However, the morphology of PPy-TiP nanocomposite (**Fig. 3c**) is exactly not same as that of PPy and TiP. PPy deposited on the surface of TiP is clearly observed, which is dense and globular. Thus, from the FTIR and FE-SEM results, it can be confirmed that the PPy polymerization has taken place on the surface of TiP. PPy-TiP nanocomposite formation is shown schematically in **Fig. 1(b)**.

The 3D surface area maps of PPy, TiP and PPy-TiP nanocomposite before and after immobilization of YADH are shown in **Figs. 4(a-c)** and **(a'-c')** respectively. It can be seen that PPy-TiP nanocomposite bears more porous and bumpy, rough surfaces than pristine PPy and TiP as shown in **Fig 6(a-c)**. Thus, PPy-TiP nanocomposite acts as a better platform for immobilization of YADH than pristine PPy and TiP. Further, a glimpse of the figures indicates that PPy, TiP and PPy-TiP nanocomposite after immobilization of YADH bear smooth surfaces due to the adherence of YADH; which suggests a successful immobilization of YADH enzyme.

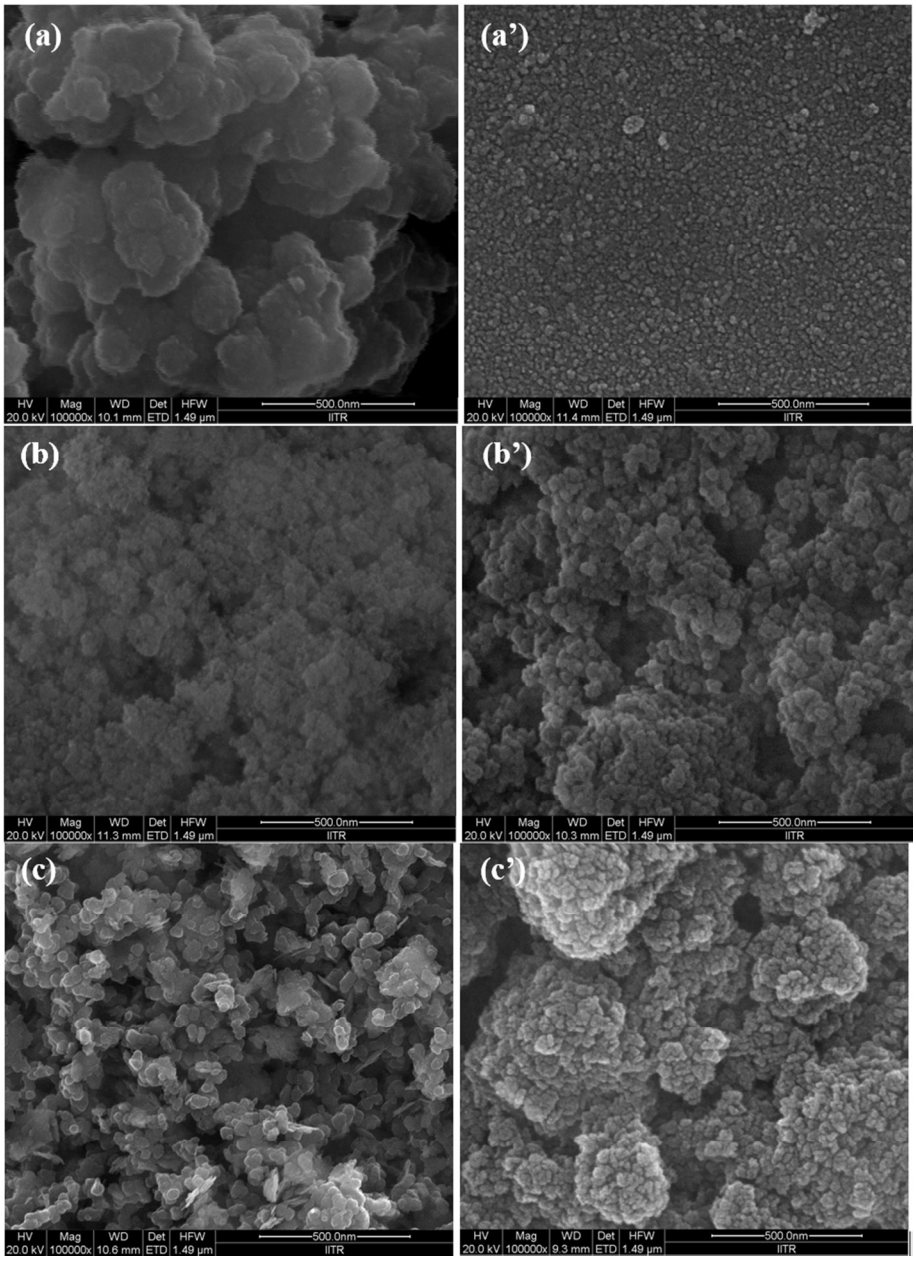

Fig. 3. Scanning electron micrographs of (a) PPy, (b) TiP, (c) PPy-TiP nanocomposite before immobilization and (a') PPy, (b') TiP, (c') PPy-TiP nanocomposite after immobilization of YADH.

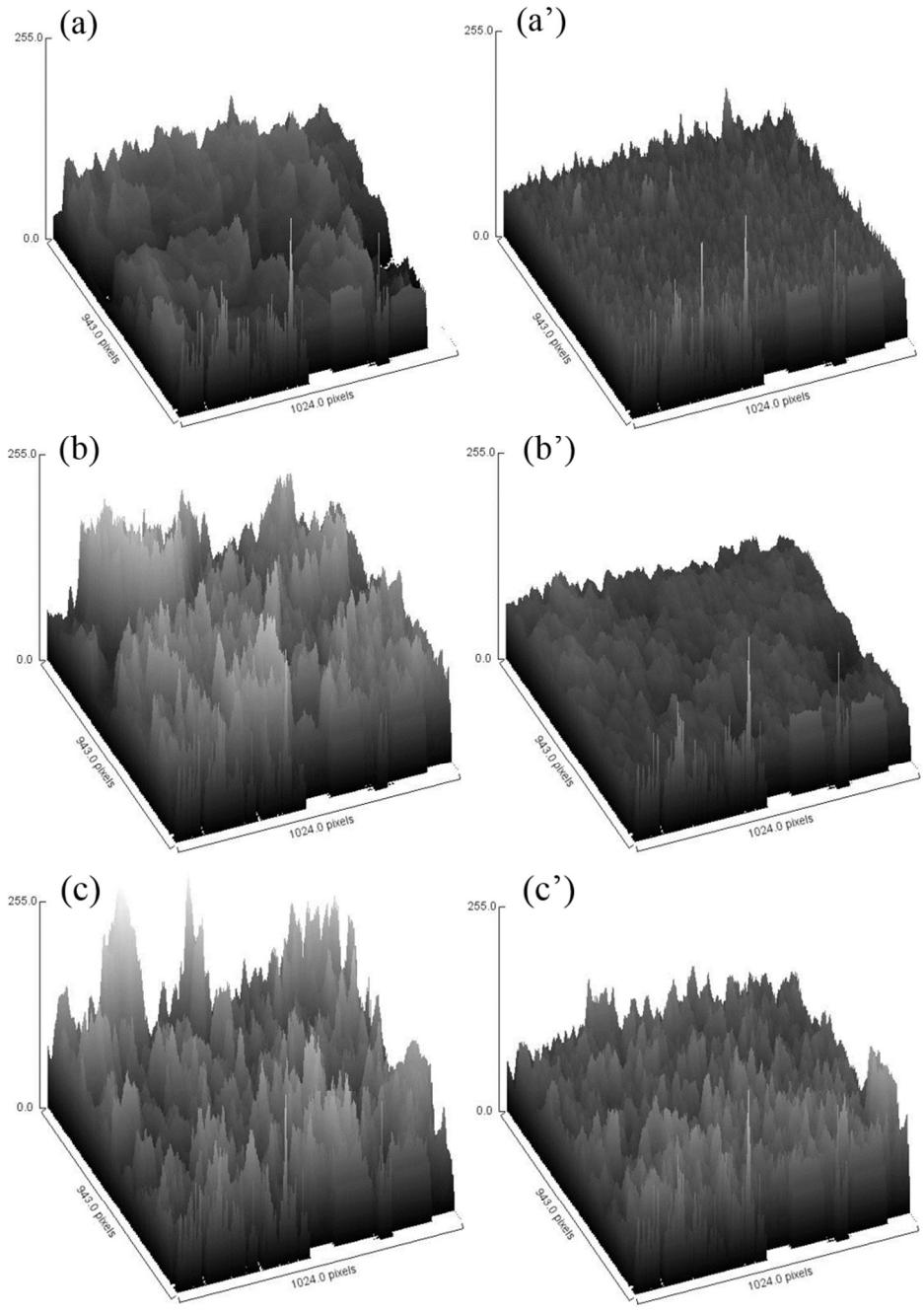

Fig. 4. 3D surface area maps of (a) PPy, (b) TiP, (c) PPy-TiP nanocomposite before immobilization and (a') PPy, (b') TiP, (c') PPy-TiP nanocomposite after immobilization of YADH.

3.3. Thermogravimetric analysis

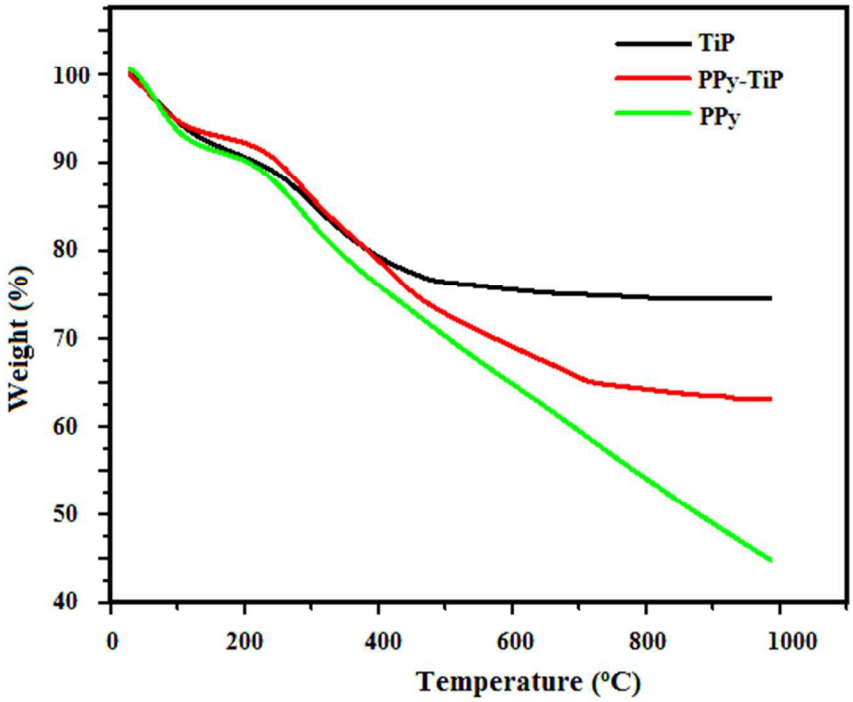

Fig. 5. TGA curves of PPy, TiP and PPy-TiP nanocomposite.

The mass losses of pure PPy, TiP and PPy-TiP nanocomposite on heating in presence of nitrogen are compared and ~~is~~ shown in **Fig. 5.** Pure PPy was found to be stable up to 200 ºC (10.27% mass loss; due to the evaporation of physically adsorbed water molecules over this temperature). Above this temperature, a gradual weight loss was observed with the similar rate till 1000 ºC (32.23% mass loss) which may be ascribed to the degradation of the unsaturated groups present in the polymer. In the case of TiP, the first weight loss was observed at 100 ºC due to removal of external water molecules and the next at 300 ºC. After 400 ºC, the TiP was found stable up to 1000 ºC. However, in case of PPy-TiP nanocomposite, the first weight loss at 150 ºC occurred due to removal of external water molecules and second weight loss up to 400 ºC occurred because of degradation of PPy. Above 700 ºC, the PPy-TiP nanocomposite remained stable up to 1000 ºC. Thus, the results in Fig. 5 indicate that PPy-TiP nanocomposite is thermally

more stable than PPy. The total mass loss up to 1000 ºC was found to be about 42.25%, 25.01% and 32.50% for PPy, TiP and PPy-TiP nanocomposite, respectively. Overall, it may be suggested that the increased thermal stability of PPy-TiP nanocomposite in comparison to PPy is due to the synergistic effect of TiP component.

3.4. Effect of temperature on the activity of soluble and immobilized YADH

The activity assay of soluble and immobilized YADH was done at different temperatures as shown in **Fig. 6**. It was observed that immobilized formulation having high residual activity at high temperature as compare to the soluble one. Immobilized YADH on TiP and PPy-TiP nanocomposite having 50% and 70% residual activity at 70 ºC respectively, whereas soluble fraction retained only 22% activity at the csame temperature. There is shift in temperature optima after immobilization of YADH, immobilized YADH shows maximum activity at 45 ºC where as soluble YADH having maximum activity at 40 ºC. Similar reports are also available on the increase in temperature optima during enzyme immobilization.[29-30] The shift in optimal temperature after immobilization of the enzyme to a support such as nanocomposite might be due to enhanced stability of the enzyme which helps in the formation of enzyme–substrate complex without altering the accessibility of substrates to the active site.[31,30] At higher temperature, the activity of both the enzyme preparations decreases due to thermal inactivation of the enzyme, but immobilized YADH was having higher activity as compared to soluble enzyme. From the results, YADH immobilized on PPy-TiP nanocomposite could lower the rate of inactivation of enzyme and make the enzyme more resistant to the change of temperature compared to the soluble YADH.

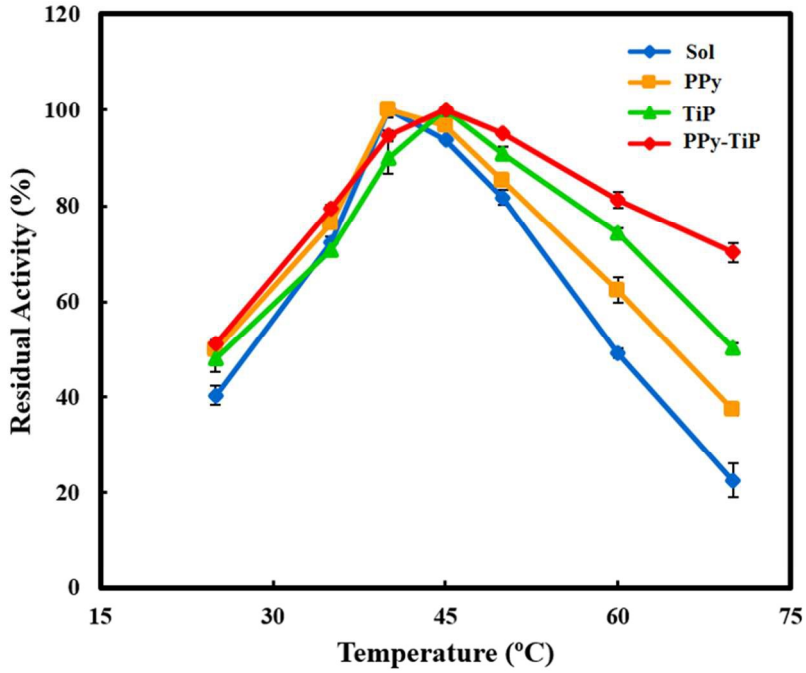

Fig. 6. Temperature activity profile of soluble and immobilized YADH. The activity of soluble and immobilized YADH was measured at various temperatures (25-70 ºC) in 0.1 M Tris-HCl buffer, pH 8.0 for 3.0 min. The enzyme activity at 45 °C was taken as a control (100%) for the calculation of remaining percent activity of soluble and immobilized enzyme. The panel denotes sol. (◆) for soluble enzyme and immobilized YADH on PPy (■), TiP (▲) and PPy-TiP (◆) respectively.

3.5. Effect of pH on the activity of immobilized YADH

In any enzymatic reaction mixture, pH is a one of the important parameter which affects the enzyme most. Therefore, we have observed the effect of pH on the activity of soluble and immobilized YADH on the TiP and PPy-TiP nanocomposite as shown in **Fig. 7.** It has been observed that there is no change of optimum pH in both the enzyme preparations, which is also reported in my previous report.[25] In general, changes in pH would directly affect the ionisable groups of amino acid residue and thereby results in unfolding of protein and subsequently loss of catalytic properties. The immobilized YADH on PPy-TiP nanocomposite was having better residual activity under extreme acidic condition (pH=3) as well as alkaline condition (pH=12)

than the soluble YADH i.e., 18% vs 65% and 6% vs 4% respectively. From the obtained results, YADH immobilized on PPy-TiP nanocomposite shows better residual activity in alkaline as well as acidic condition. This enhanced activity might be attributed to the presence of ionisable group on the support and strong covalent bond between enzyme and support.

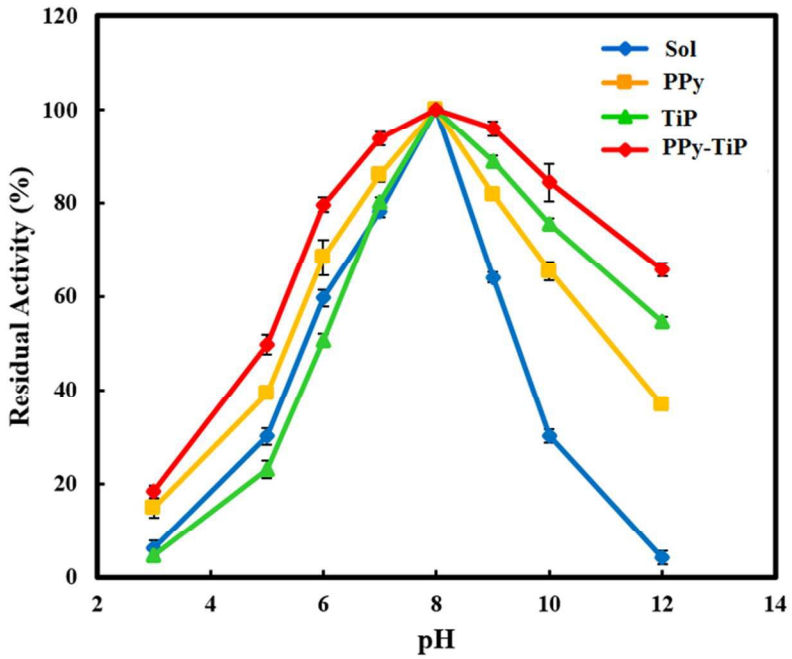

Fig. 7. pH activity profile of soluble and immobilized YADH. The activity of soluble and immobilized YADH was measured in the buffers of various pH (3.0-12.0). The used buffers were glycine-HCl (pH 3.0), sodium acetate (pH 5.0), sodium phosphate (6.0, 7.0), Tris-HCl (pH 8.0, 9.0) and glycine-NaOH (pH 10.0, 12.0) and molarity of each buffer was 0.1 M. The activity at pH 8.0 was chosen as a control (100%) for the calculation of remaining percent activity. The panel denotes sol. (◆) for soluble enzyme and immobilized YADH on PPy (■), TiP (▲) and PPy-TiP (◆) respectively.

Because PPy-TiP nanocomposite is having permanent negative charge on the phosphate group of TiP, this may cause partitioning of protons, which attract the protons (lowering the pH) around the enzyme.[32] Same results also follow in the case of acidic region where pyrrole residue having lone pair, which bind excess of hydride ion (H^+) present in the solution, thus preventing H^+ diffuse into the inner polymer matrix and attracting with enzyme. In this way, the pH change

in the microenvironment was envisage to be smaller than that in the bulk solution. Therefore nanocomposite act as a dual system like buffers. In this way, effects of pH is nullified by the matrix to some extent.[33]

3.6. Thermal stability analysis

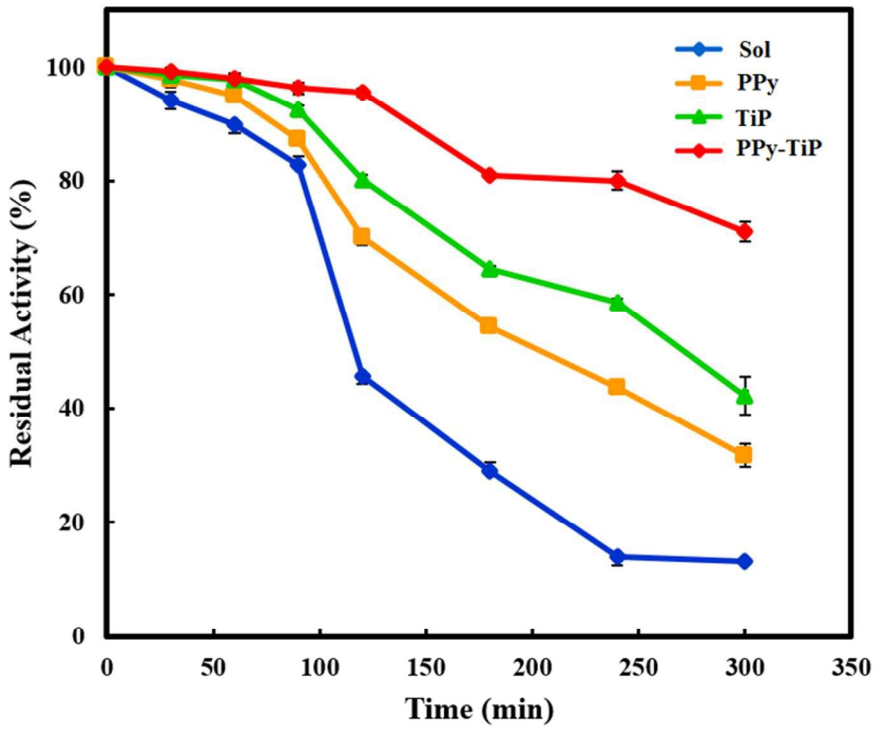

Fig. 8. Thermal denaturation profile of soluble and immobilized YADH. Soluble and immobilized YADH was incubated at 60 °C in 0.1 M Tris-HCl buffer of pH 8.0 for varying time. Aliquots of each preparation were carried out at a particular interval of time and chilled quickly in ice for 5 min. The activity of the enzyme obtained without incubation at 60 °C as taken as a control (100%) for the calculation of remaining percent activity. The panel denotes sol. (◆) for soluble enzyme and immobilized YADH on PPy (■), TiP (▲) and PPy-TiP (◆) respectively.

The analysis of thermal stability was done for both free and immobilized YADH following the incubation of the enzyme preparations at 50 ºC for a period of 300 minutes and measuring their residual activity. From the **Fig. 8** it is observed that soluble and adsorbed YADH retained 13% and 32% activity after 300 minutes of incubation at 50 ºC respectively, whereas

PPy-TiP nanocomposite bound YADH retained 71% residual activity under the similar incubation condition. The improved thermal stability of immobilized YADH may be provided by PPy-TiP nanocomposite matrix, which absorbs some heat of the system and shield the enzyme from thermal denaturation. It also believed that immobilization of YADH on PPy-Tip nanocomposite, which provide rigidity and compactness to the YADH and prevent undesirable change in the tertiary structure to this enzyme.[34]

3.7. Reusability

It is an important parameter of any enzymes for the potential industrial applications. To investigate the reusability of the immobilized YADH was examined by using the same system repeatedly ten times within ten days, and the results exhibited that Ppy-TiP nanocomposite bound YADH enzyme retained 75% residual activity as compare to the YADH adsorbed on PPY which retained only 40% of its residual activity after ten repetitive use (**Fig. 9**). There was no significant decrease in the residual activity of immobilized YADH upon several uses. The results signify that YADH immobilized on PPy-Tip nanocomposite having good durability and also leakage of the protein is minimum as compare to PPy polymer alone. (See supplementary Table S2)

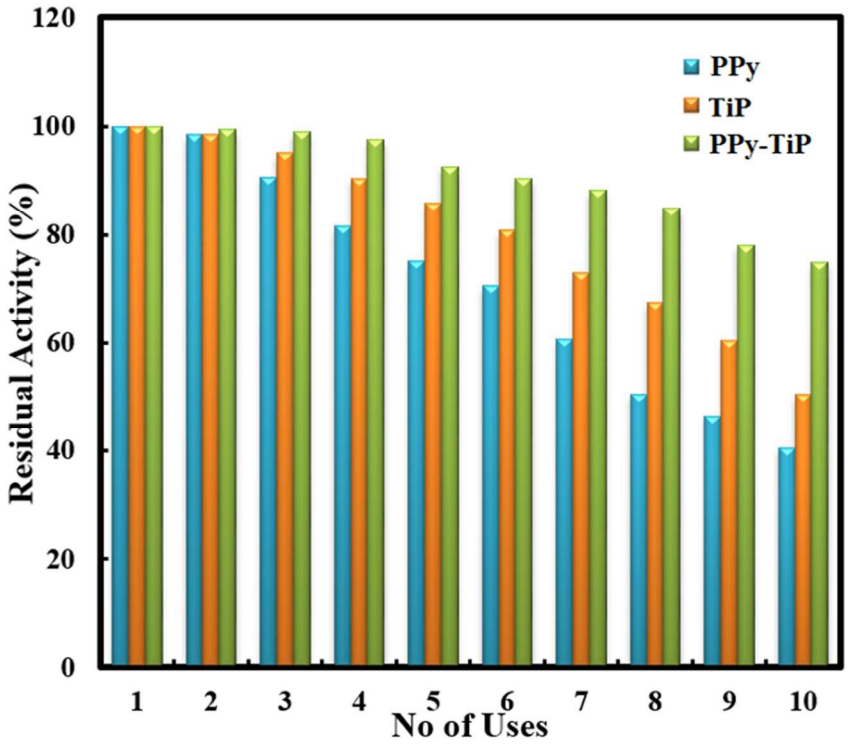

Fig. 9. Reusability of immobilized YADH. Reusability of immobilized YADH monitors for 10 successive days. The activity calculated on first day taken as a control (100%) for the calculation of the remaining activity after each use. The panel denotes sol. (◆) for soluble enzyme and immobilized YADH on PPy (■), TiP (▲) and PPy-TiP (●) respectively.

3.8. Kinetic parameter of soluble and immobilized YADH

For the kinetic parameter analysis for the soluble and immobilized YADH we were used ethanol as a substrate. To determine the efficiency of YADH after immobilization, we have calculate the velocity maximum (Vmax) and Michaelis-Menton constant (Km) of the immobilized YADH on PPy-TiP nanocomposite and compared with soluble YADH. Vmax and Km of soluble and immobilized YADH were calculated by Lineweaver Burk plot (**Fig. 10**).

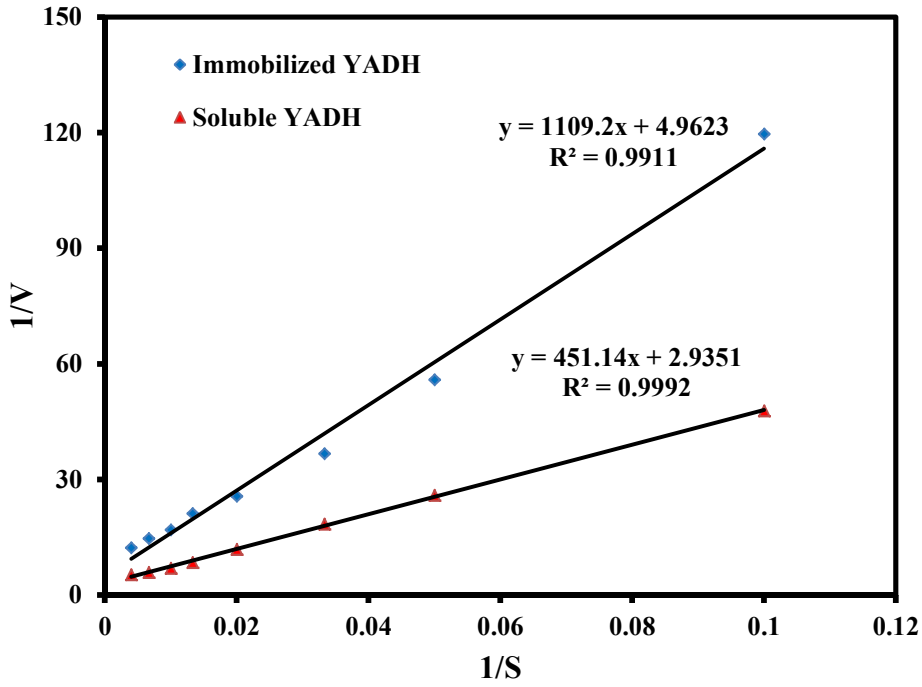

Fig. 10. Double reciprocal plot for oxidation of ethanol by soluble and immobilized YADH.

As it has been observed from the **Table 1** that Km of the YADH increases after immobilization on PPy-TiP nanocomposite, which might be due to hindrance caused by the nanocomposite to the substrate that resulted in dercrease in the diffusion rate of substrate to the active site of enzyme. Increase in Km was previously reported for YADH when immobilized by covalent linkage, encapsulation and adsorption to the various matrices like nanocrystalline Cu-Ni nanoferrite, polymer-inorganic hybrid microcapsule, glyoxal-agarose, and silica nanotubes-doped alginate gel etc.[25, 29, 35-36] The maximum reaction rate of the immobilized YADH is lower than that of soluble YADH. The immobilized YADH retained 59.15% enzymatic activity compared to soluble enzyme. The decreased Vmax of immobilized YADH may be attributed to the conformational alterations in the enzyme after immobilization with PPy-TiP nanocomposite which directly affects the binding propensity of the NAD^+ and ethanol to the immobilized YADH.

Table. 1. The kinetic parameters for soluble and immobilized YADH

Alcohol dehydrogenase	Km (mM)	Vmax(µmol min^{-1})	Vmax /Km	Relative activity (%)
Soluble	153.6	340.7	2.218	100
Immobilized	223.71	201.53	0.901	59.15

The present immobilization strategy is compared with some of the published methods [37-40,] for YADH as shown in **Table 2.** It has been observed that the immobilization of YADH on PPy-TiP nanocomposite improved its activity, stability and reusability compared to earlier reports.

Table 2. Comparison of immobilized YADH on nanoparticles by different methods.

Methods	Immobilization efficiency (%)	Optimum pH	Optimum Temperature	References
YADH immobilized on magnetic nanoparticles	48.77	6.8-8.0	40 °C	[37]
YADH/ Fe_3O_4 NPs using carbodiimide as linker	62	5.0-6.0	50 °C	[38]
YADH immobilized on hybrid Alginate- chitosan beads	62.76	7.0	40 °C	[39]
YADH immobilized on chitosan coated magnetic Nanoparticles	65	7.4	30 °C	[40]
YADH immobilized on PPy-TiP nanocomposites	69	8.0	45 °C	Present method

3.9. In-silico screening

Molecular docking studies were carried out to identify methods to explain the obtained YADH results. Hence, YADH data of PPy, activated TiP and activated PPy-TiPnanocompositewere investigated on a structural basis, as well as by molecular modeling and a docking study against the yeast alcohol dehydrogenase (3BTO; pbd) using MVD and Discovery studio software to predict the affinity, orientation and surrounding surface (Fig. 11) of the PPy, activated TiP and activated PPy-TiP nanocomposite at the active site (i.e. allosteric sites). The secondary forces were in good agreement with the predicted binding affinities obtained by molecular docking studies, as verified by YADH studies showing the activated PPy-TiP nanocomposite (Fig. 11c) to be the most active among the PPyand activated TiP (Fig. 11a and 11b). On the basis of the obtained Km values (see section; 3.8. Kinetic parameter of soluble and immobilized YADH), it is pertinent to mention that the function of docking site was reported as allosteric sites,[41-44] not an active site of enzyme activity. If the enzyme active sites are the same as the docking sites, then the value of Km decreases, however, in our case, the value of Km increases. This regression in Km values decreases the catalytic action of the enzyme and/or in some cases, even stops catalysis. Since, there is no competition between the substrate and substance for occupying active sites of enzyme, PPy, TiP or PPy-TiP was successfully docked at allosteric sites of 3BTO, respectively. This fact is strengthened by the experimental values of Km. A slight increment in the km value as compare with soluble YADH shows no major alteration in the active site of the enzyme responsible for the catalytic reaction. The immobilization of the enzyme to support such as nanocomposite might be due to enhanced stability of the enzyme which helps in the formation of enzyme–substrate complex without altering the accessibility of substrates to the active site.

The stability of the enzyme is primarily focused; therefore, small changes in the affinity are nullified by the stability of the enzyme because YADH is an industrially important enzyme.

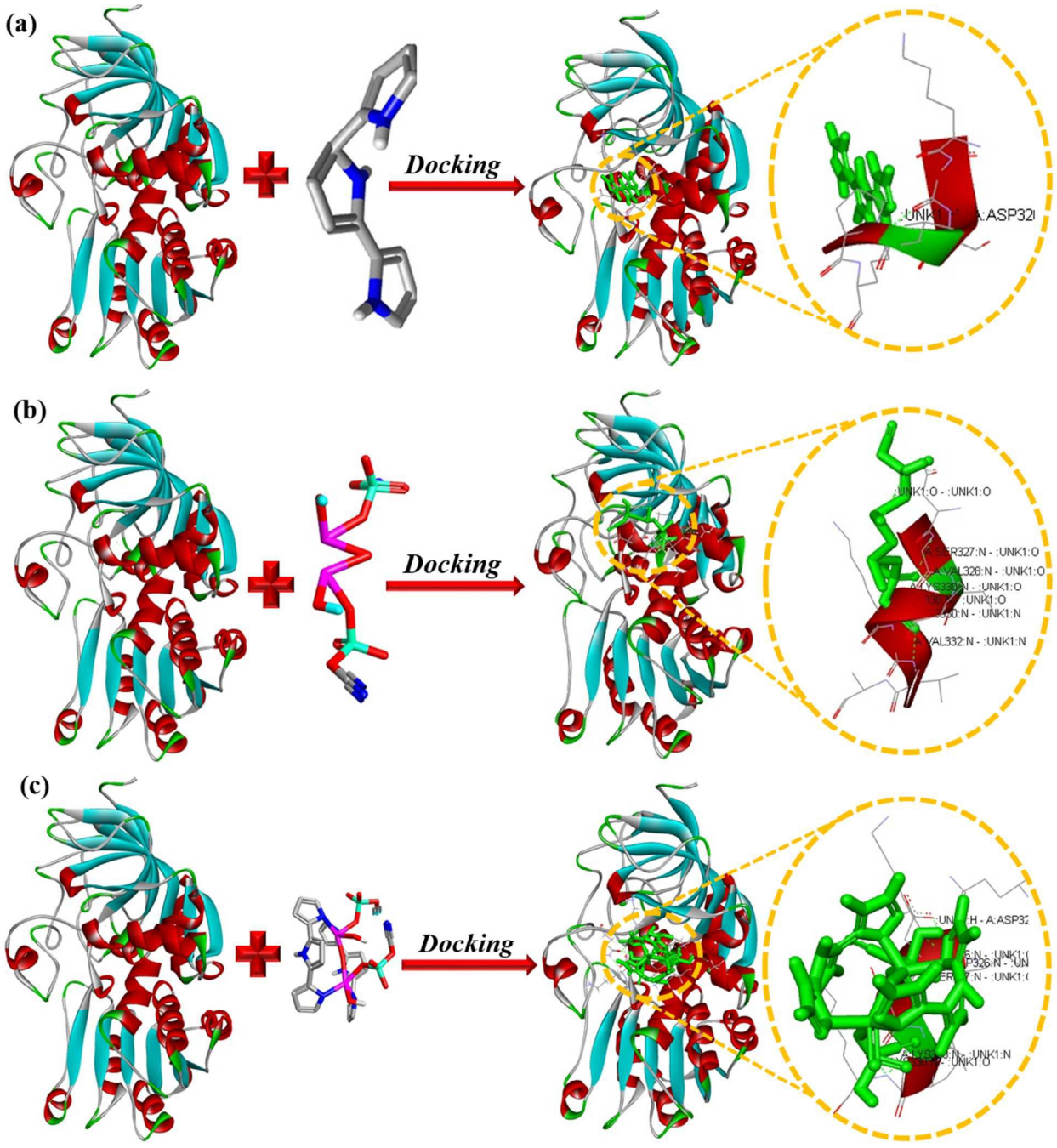

Fig. 11. The binding mode of (a) PPy, (b) TiP and (c) PPy-TiP nanocomposite into the active site of the receptor (3BTO; pdb) displaying secondary bonds as shown encircled (The inset shows the site of unit A with the bound PPy, TiP and PPy-TiP).

Based on the molecular docking studies, the ASP326:N-:UNK1:O with three interaction of same residue, SER327:N-:UNK1:O, SER327:N-:UNK1:O, LYS330:N-:UNK1:O, LYS330:N-:UNK1:N and UNK1:H-ASP326:OD1 residues (Fig. 11c) interacted with the activated PPy-TiP in the proper orientation and comparatively high frequency when compared to the PPy and TiP. The binding energy for the PPy, activated TiP and activated PPy-TiP nanocomposite were estimated to be -78.349, -95.746, -100.085 kcal/mol, respectively. The force operating in the docking simulation is primarily associated with hydrogen bonding, electrostatic forces, van der Waals forces, and hydrophobic interactions. As shown in Fig. 12, the activated PPy-TiP nanocomposite demonstrated better affinity to receptors and showed better docking scores as it was buried well inside the cavity of the target YADH because of the combined effect of the PPy and activated TiP. The interaction results showed the activated PPy-TiP nanocomposite was suitable for the immobilization of enzyme. As a new support, activated PPy-TiP nanocomposite effectively increases the stability of enzyme, permitted the reuse or continuous use of enzymes and thus improved usability in practice.

3.10. Field points of PPy, activated TiP and activated PPy-TiP nanocomposite

Fields points consist of the electrostatic, van der Waals and hydrophobic potentials of the molecule and may be considered as extended information of pharmacophores, with the advantages that their position is directly calculated from the molecule's physical properties, and they have size/strength information associated with them and categories the nature and capability of bonding with ligand-receptor interaction effects so that e.g. not all H-bond donors are treated the same: some make stronger bonds than others. The four field point patterns are used to express the simultaneous operation of all potential interactions that a field points of PPy,

activated TiP and activated PPy-TiP nanocomposite in a specified conformation can make to a receptor ligands connections as shown in Fig. 12. (A representative field point pattern is shown in Fig. 12) Larger field points are indicative of the strong points of potential interaction. Moreover, Geometrical descriptor of the PPy, TiP and PPy-TiP nanocomposite were also used to show the extent of the surface interaction of the mentioned synthesized compounds (Fig. 13).

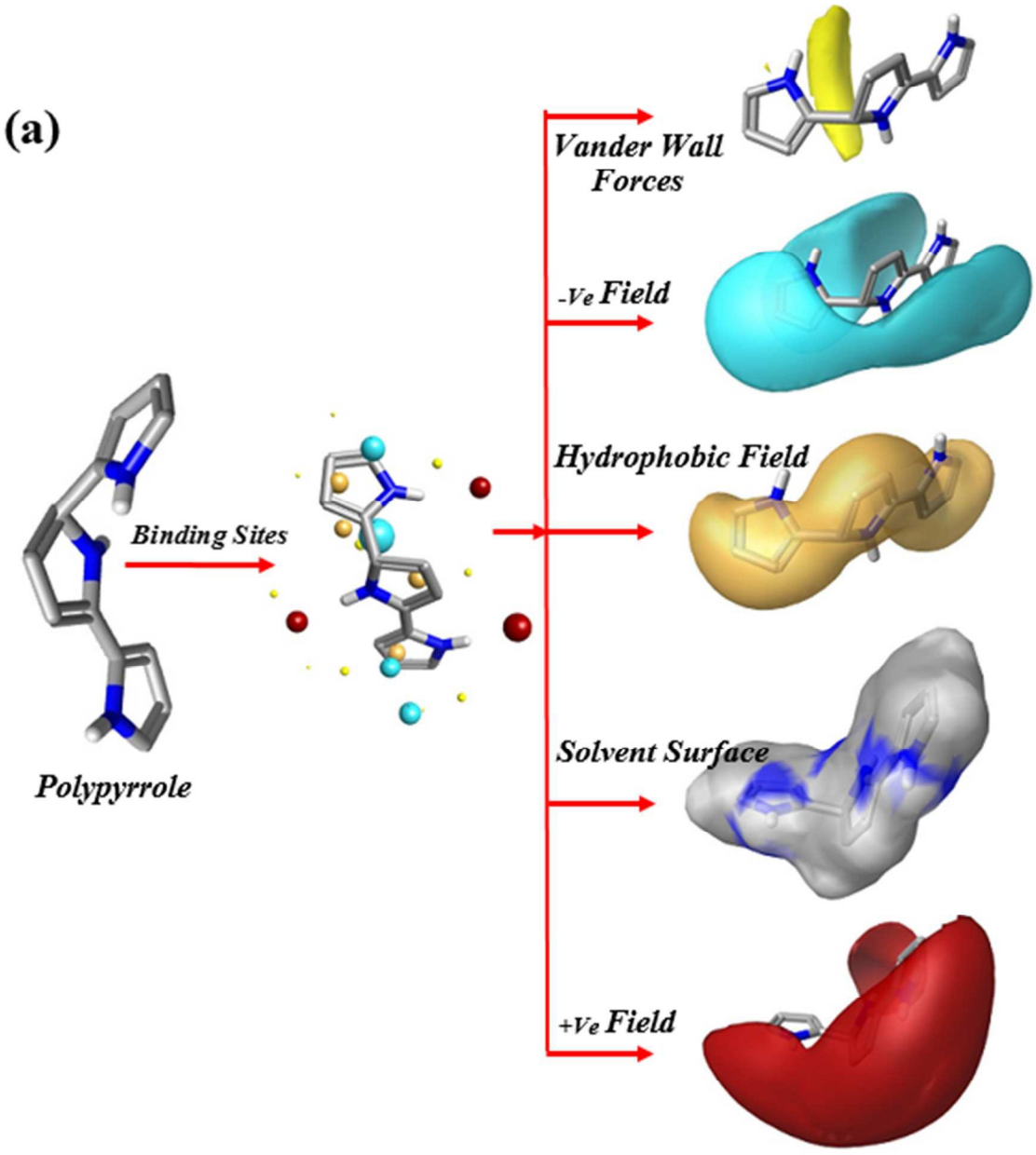

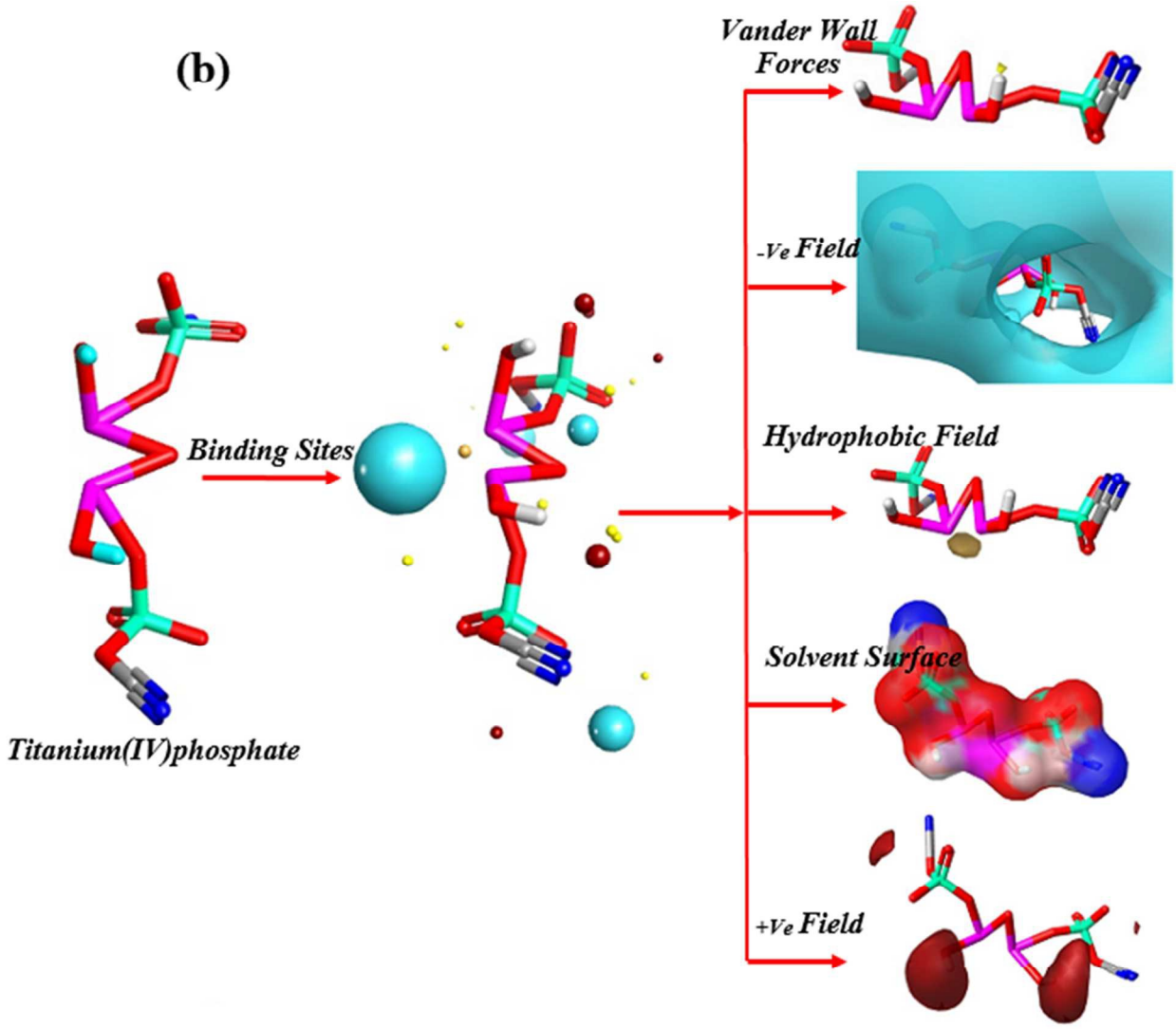

1

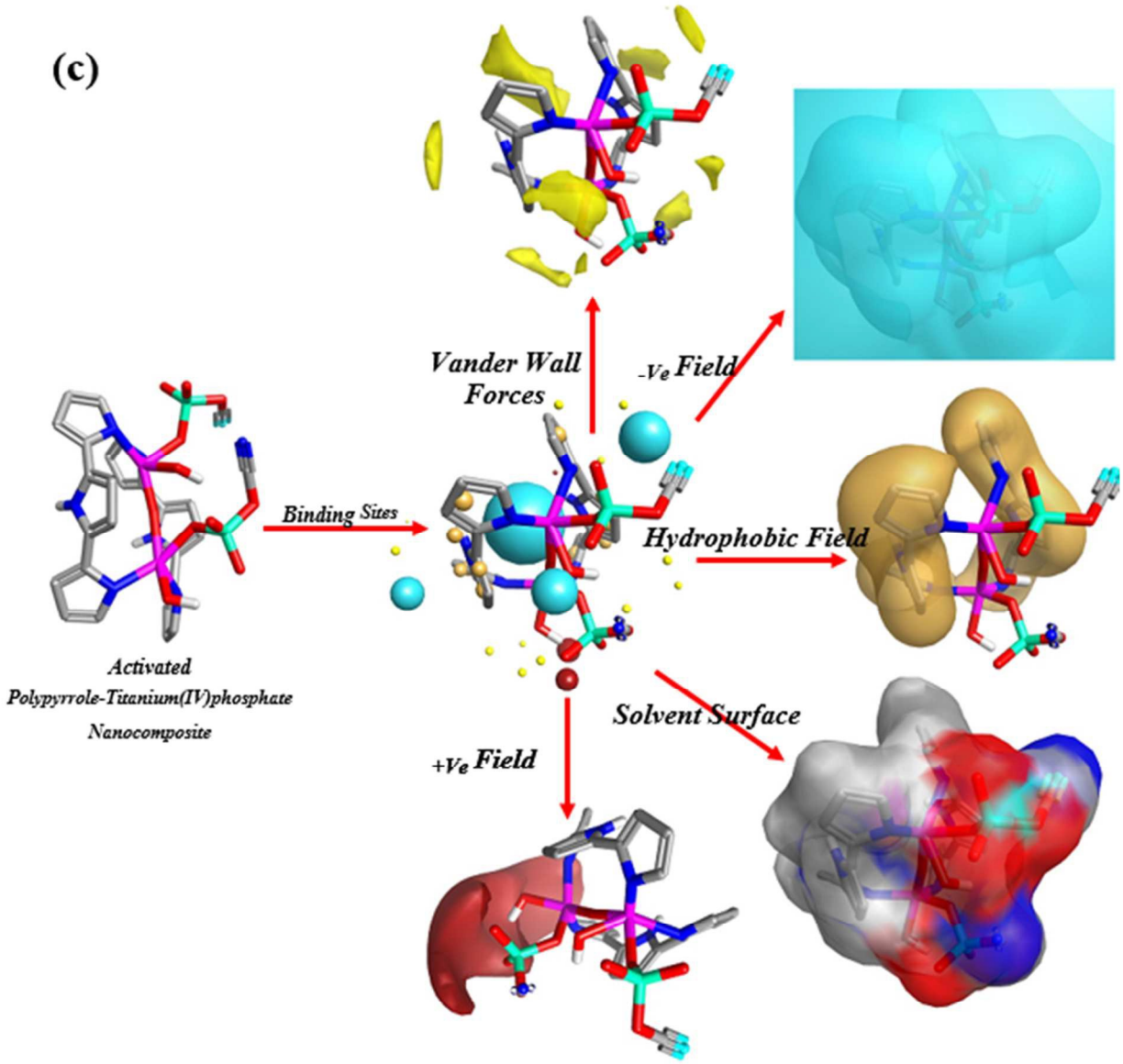

Fig. 12. Interpretation of a field point pattern of the expected (a) PPy, (b) TiP and (c) PPy-TiP nanocomposite (The size of the point indicates the potential strength of the interaction); Blue: negative field points (like to interact with positives/H-bond donors on a protein); Red: positive field points (like to interact with negatives/H-bond acceptors on a protein); Yellow: van der Waals surface field points (describing possible surface/vdW interactions) and Gold/Orange: hydrophobic field points (describe regions with high polarizability/hydrophobicity). (For interpretation of the references to color in this figure legend, the reader is referred to the web version of this article)

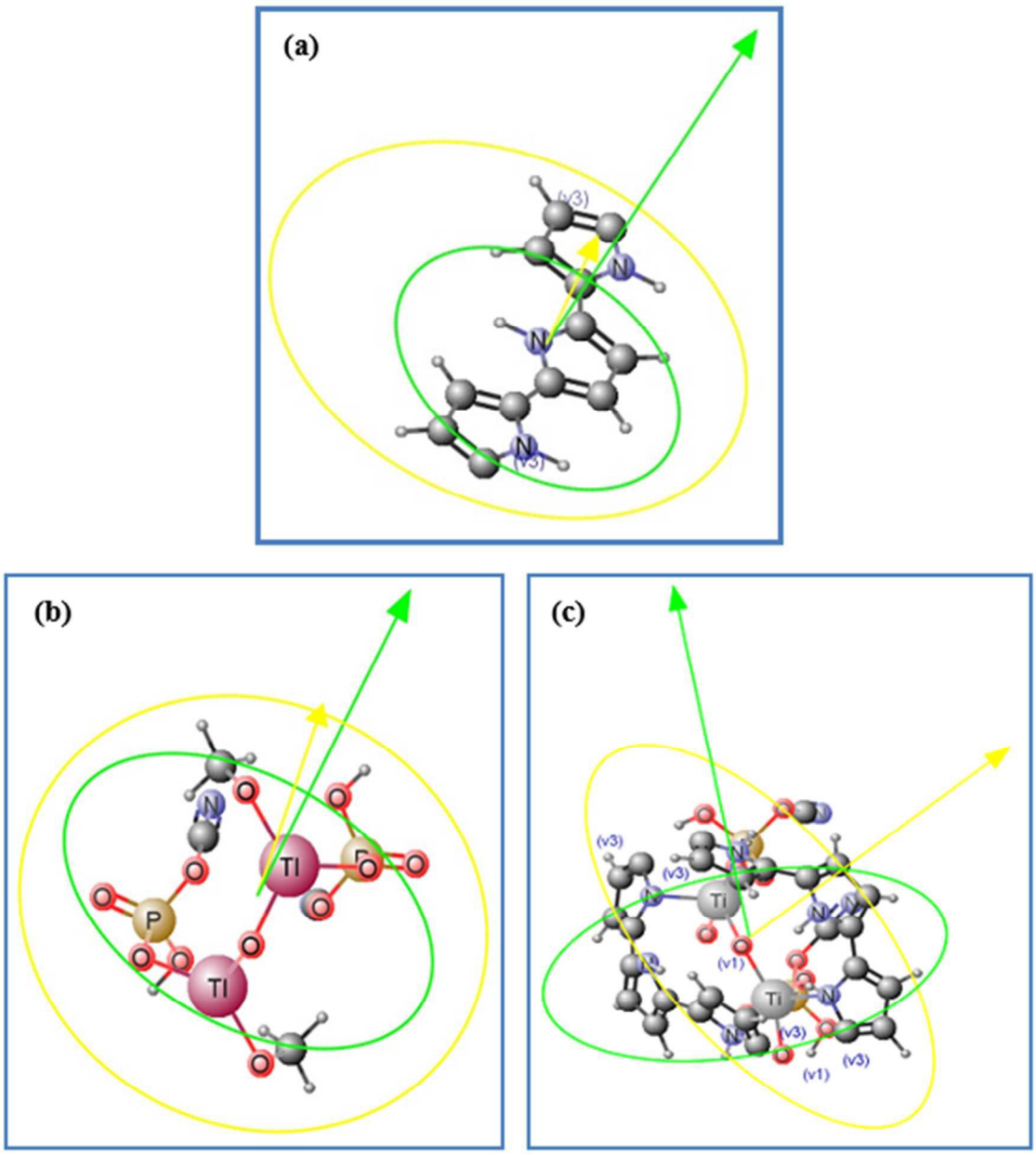

Fig. 13. Geometrical structure of a PPy (a), TiP (b), and PPy-TiP nanocomposite (c) showing Van der Waals volume and length perpendicular to the maximum and minimum area.

4. Conclusion

Yeast alcohol dehydrogenase was successfully immobilized on polypyrrole-titanium(IV)phosphate nanocomposite. Comparative study was done in terms of resistance to pH

and temperature, thermal stability, storage stability, reusability and recovery. Significant improvement was found in terms of all the parameters for yeast alcohol dehydrogenase immobilized on polypyrrole-titanium(IV)phosphate nanocomposite compared to YADH immobilized on titanium(IV)phosphate, polypyrrole and the free YADH. Such strategy of immobilization of yeast alcohol dehydrogenase on polypyrrole-titanium(IV)phosphate nanocomposite may contribute to the favourable use of the enzyme in industry-based applications. The structure-based docking simulation was demonstrated to help investigate the binding modes between the appropriate amino acids of the yeast alcohol dehydrogenase and chemical entities. This strategy successfully predicts the interaction between enzyme and nanocomposite. Furthermore, the hydrogen bond and van der Waals interactions were also found to play a key role in forming energetically favored complex. The docking result of the reported enzyme activity was consistent with the experimental results.

Acknowledgement

The support of this work by KFUPM through the project # R15-CW-11 (MIT-13103, 13104) under the Center of Excellence for Scientific Collaboration with MIT is gratefully acknowledged.

Electronic Supplementary Information

Supporting information includes loading efficiency of varying amount of YADH added to nanocomposite, enzyme leakage behavior, effect of temperature and effect of pH on the activity of soluble and immobilized YADH.

References:

1. X. Feng, N. Chen, J. Zhou, Y. Li, Z. Huang, L. Zhang, Y. Ma, L. Wang, X. Yan, *New J. Chem.*, 2015, **39**, 2261-2268.

2. J. Wei, G. Xing, L. Gao, H. Suo, X. He, C. Zhao, S. Li, S. Xing, *New J. Chem.,* 2013, **37**, 337 341.

3. C. Guo, X. Yang, X. Wang, M. Pei, G. Zhang, *New J. Chem.*, 2013, **37**, 4163-4169

4. U. Baig, R.A.K. Rao, A.A. Khan, M.M. Sanagi, M.A. Gondal, *Chem. Eng. J.,* 2015, **280**, 494-504.

5. R. Karthik, S. Meenakshi, *Int. J. Biol. Macromol.,* 2015, **72**, 711-717.

6. U. Baig, W.A. Wani, L.T. Hun, *New J. Chem.,* 2015, In Press, DOI: 10.1039/C5NJ01029B.

7. A.A. Khan, U. Baig, *Composites: Part B,* 2014, **56**, 862-868.

8. A.A. Khan, U. Baig, *Sens. Actuators, B,* 2013, **177**, 1089-1097.

9. M. Shakir, N. e. Iram, M. S. Khan, S. I. Al-Resayes, A. A. Khan, U. Baig, *Ind. Eng. Chem. Res,* 2014, **53**, 8035-8044.

10. A. Arslan, S. Kiralp, L. Toppare, Y. Yagci, *Int. J. Biol. Macromol.,* 2005, **35**, 163-167.

11. S. Tirkes, L. Toppare, S. Alkan, U. Bakir, A. Onen, Y. Yagcı, *Int. J. Biol. Macromol.,* 2002, **30**, 81-87.

12. J.K. Mathod, R.M.V.K. Rao, *Polym. Composites,* 2011, **32**, 1416-1422.

13. A. Bhaumik, S. Inagaki, *J. Am. Chem. Soc.* 2001, **123**, 691-696.

14. H. Jornvall, B. Persson, J. Jeffery, *Eur. J. Biochem.* 1987, **167**, 195-201.

15. V. Leskovac, S. Trivic, D. Pericin, *FEMS Yeast Res.* 2002, **2**, 481-94.

16. S. Panke**,** M. Held, and M. Wubbolts, *Curr. Opin. Biotechnol.* 2004, **15**, 272-279.

17. A. Schmid, J. S. Dordick, B. Hauer, A. Kiener, M. Wubbolts, and B. Witholt, *Nature* 2001, **409**, 258-268.

18. H. Schoemaker, H. E., D. Mink, and M. G. Wubbolts, *Science* 2003, **299**, 1694-1697.

19. B. Leca, J, Marty, *Biosens Bioelectron* 1997, **12**, 1083-1088.

20. S.B. Jadhav, S.B. Bankar, T. Granström, H. Ojamo, R.S. Singhal, S.A. Survase, *Appl Microbiol Biotechnol.* 2014, **98**, 6307-16.

21. G.Y. Li, K.L. Huang, Y.R. Jiang, D.L. Yang, P. Ding. *Int. J. Biol. Macromol.*, 2008, **42** 405-412.

22. C.O. Fagain, *Enzy. Micr. Technology*, 2003, **33**, 137-149.

23. R.K. Singh, M.K. Tiwari, R. Singh, J.K. Lee. *Int. J. Mol. Sci.*, 2013, **10**, 1232-1277.

24. C. Mateo, J.M. Palomo, G.F. Lorente, J.M. Guisan, *Enzy. Microb. Tech.,* 2007, **40**, 1451-1463.

25. M. Shakir, Z. Nasir, M.S. Khan, Lutufullah, M.F. Alam, H. Younus, S.I, Al-Resayes, *Int. Biol. Macromol.,* 2015, **72**, 1196-1204.

26. A. Khan and U. Baig, *J. Hazard. Mater.,* 2011, **186**, 2037-2042.

27. A. Khan and U. Baig, *J. Ind. Eng. Chem.,* 2013, **19**, 1226-1236.

28. A. Panjkovich, X. Daura, *Bioinformatics* 2014, **30**, 1314-1315.

29. M.H. Liao, D.H. Chen, *Biotechnolo. Lett.*, 2001, 23, 1723-1727.

30. N. Ortega, M. Perez-Mateos, *J. Agric. Food Chem.,* 2009, 57, 109-115.

31. R.S. Rao, P.S. Borkar, C.N. Khobragade, A.D. Sagar, *Enzyme. Microb. Tech,* 2006, **39** 958-962.

32. Q. Zhao, Y. Hou, G.H.Gong, M.A.Yu, L. Jiang, F. Liao, *Appl. Biochem. Biotechnol.,* 2010, **160,** 2287-99.

33. X. Song, H. Wu, J. Shi, W. Zhang, Q. Ai, Z. Jiang, *J. Mol. Catal. B: Enzym.,* 2014, **100**, 49-58.

34. S.C. Tsang, C.H. Yu, X. Gao, K. Tam**,** *J. Phys. Chem. B,* 2006, **110**, 16914-22.

35. S. Xu, Y. Lu, Z. Jiang, H. Wu, *J. Mol. Catal. B: Enzym.,* 2006, 43, 67-73.

36. L. Zhang, Y. Jiang, J. Shi, X. Sun, J. Li, Z. Jiang, *React. Funct. Polym.,* 2008, **68,** 1507-1515.

37. G.Y. Li, K.L. Huang, Y.R. Jiang, D.L. Yang, P. Ding, *Int. J. Biol. Macromol*., 2008, **42,** 405-412.

38. M.H. Liao, D.H. Chen, *Biotechnol. Lett., 2001,* **23**, 1723-1727.

39. Z.D. Zhou, G.Y. Li, Y.J. Li, *Int. J. Biol. Macromol*., 2010, **47**, 21-26.

40. G.Y. Li, Z.D. Zhou, Y.J. Li, K.L. Huang, M. Zhong, *J Magn. Magn. Mater*., 2010, **322**, 3862-3868

41. J.Y. Lee, K.W. Jung, E.R. Woo, Y. Kim, *Bull. Korean Chem. Soc.,* 2008, **29**, 1479-1484.

42. J. A. Hardy, J. A. Wells, *Curr. Opin. Struct. Biol*. 2004, **14**, 1-10

43. Y. Tokunaga**,** K. Takeuchi, H.Takahashi**,** I. Shimada**,** *Nat. Struct. Mol. Biol.,* 2014, **21**, 704-711.

44. U. D. Ramirez, F. Myachina, L. Stith, E. K. Jaffe, *Adv. Exp. Med. Biol.,* 2010, **680**, 481-488.

For TOC

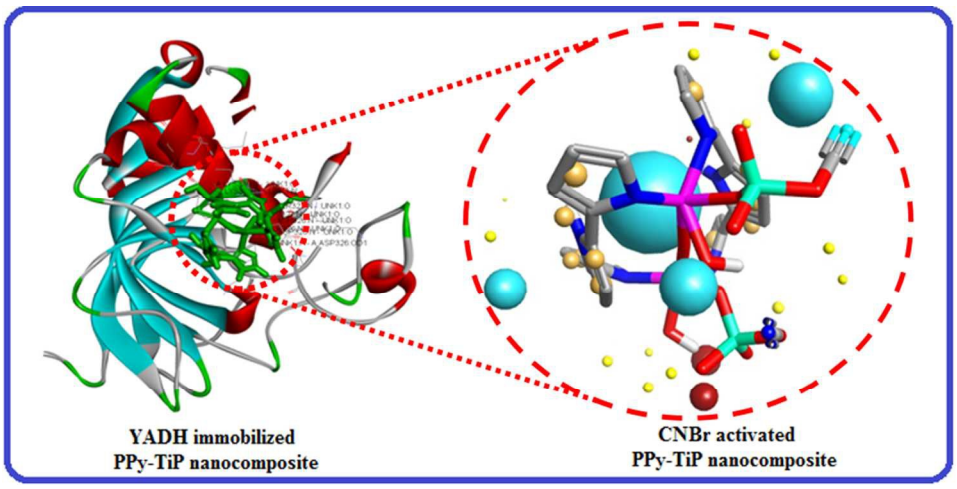

Polypyrrole-titanium(IV)phosphate nanocomposite was synthesized by using facile chemical oxidative polymerization of pyrrole in the presence of titanium(IV)phosphate for YADH immobilization.